Impact of La Niña on the Following-Summer East Asian Precipitation through Intermediate SST Anomalies

Na Wen, Laurent Li

▶ **To cite this version:**

Na Wen, Laurent Li. Impact of La Niña on the Following-Summer East Asian Precipitation through Intermediate SST Anomalies. Journal of Climate, 2023, 36 (17), pp.5743-5755. 10.1175/JCLI-D-22-0650.1 . hal-04294036

HAL Id: hal-04294036
https://hal.science/hal-04294036v1

Submitted on 16 Jan 2025

HAL is a multi-disciplinary open access archive for the deposit and dissemination of scientific research documents, whether they are published or not. The documents may come from teaching and research institutions in France or abroad, or from public or private research centers.

L'archive ouverte pluridisciplinaire **HAL**, est destinée au dépôt et à la diffusion de documents scientifiques de niveau recherche, publiés ou non, émanant des établissements d'enseignement et de recherche français ou étrangers, des laboratoires publics ou privés.

Distributed under a Creative Commons Attribution 4.0 International License

Impact of La Niña on the Following-Summer East Asian Precipitation through Intermediate SST Anomalies

NA WEN[a] AND LAURENT LI[b]

[a] College of Atmospheric Sciences, Nanjing University of Information Science and Technology, Nanjing, China
[b] Laboratoire de Météorologie Dynamique, CNRS, Sorbonne Université, Ecole Normale Supérieure, Ecole Polytechnique, Paris, France

(Manuscript received 27 August 2022, in final form 23 April 2023, accepted 25 April 2023)

ABSTRACT: This study investigates the impact of boreal winter–peaked La Niña on the following-summer precipitation in East Asia through intermediate sea surface temperature (SST) anomalies playing the role of relay in observation and numerical models. There are widespread dry conditions in both North and South China and wet conditions in coastal areas of central and eastern China. Such a pattern is mainly attributed to an anomalous low pressure over the western tropical Pacific and an anomalous anticyclone over northeast Asia. It is found that the delayed impact of La Niña on the East Asian climate is operated through intermediate SST anomalies—the Z-shape cold SST anomalies in the tropical North Pacific. There might be three ways for the SST anomalies to operate. First, they produce tropical atmospheric perturbations that can penetrate into the subtropical jet through the westerly trough over the northeast subtropical Pacific, the wave train being then excited along the jet. Second, perturbations created through the monsoon trough over the western Pacific can directly stimulate northward-propagating Rossby waves along the East Asian coast, mainly at low level. And third, perturbations over the tropical Atlantic–northwest Africa can also trigger downstream propagating waves along the subtropical jet. The observation effects of the intermediate SST anomalies and their possible impact mechanisms on atmospheric circulation are largely reproduced within numerical simulations performed with the Community Earth System Model.

KEYWORDS: Asia; Atmosphere-ocean interaction; La Niña; Precipitation; Sea surface temperature

1. Introduction

El Niño–Southern Oscillation (ENSO) is the most remarkable phenomenon in the tropical Pacific at interannual time scale and has a huge influence on global climate. Its positive phase, El Niño, attracts a lot of scientific interest and public awareness. El Niño exerts influences not only in its peak time in boreal winter but also in its decaying stage in the subsequent summer (Rasmusson and Carpenter 1982; Ropelewski and Halpert 1987). As a regional manifestation, East Asia shows excessive precipitation in the middle and lower reaches of the Yangtze River in summer following El Niño (Zhang et al. 1999; Chang et al. 2000; Wang and Zhang 2002; Wu et al. 2009; Wen and Hao 2021). Since sea surface temperature (SST) anomalies directly related to El Niño are largely reduced or even entirely disappear in the following summer, intermediate players must intervene to relay effects of winter-peaked El Niño. The atmospheric response to underlying surface anomalies is very fast, within only a few days or weeks (Hoskins and Karoly 1981; Peng and Whitaker 1999; Li and Conil 2003), and the East Asian summer monsoon change can only be a quasi-simultaneous response to summer SST anomalies. Several hypotheses, which all used intermediate SST anomalies in other oceanic basins to explain the delay effect of El Niño, were proposed in the literature, such as those involving local air–sea interaction sustaining the Philippine Sea anticyclone (PSAC; Wang et al. 2002, 2003), the "recharge and discharge" effect of the tropical Indian Ocean (Yang et al. 2007; Xie et al. 2009), and the possible bridging role of the tropical Atlantic SST anomalies (Rong et al. 2010).

La Niña is the antiphase of El Niño in the ENSO cycle but not its simple mirror. There are asymmetries in many aspects, such as amplitude, event evolutional course, and associated atmospheric responses (Zhou et al. 2014; McPhaden and Zhang 2009; Dommenget et al. 2013; Okumura 2019). The center of the La Niña SST anomaly is usually westward shifted, relative to that of El Niño, and with weaker amplitude (Kang and Kug 2002). This was believed to be the consequence of SST nonlinear advection in the equatorial eastern Pacific (An and Jin 2004; Su et al. 2010) or nonlinear atmospheric processes including the asymmetrical wind stress feedback over the equatorial central Pacific (Kang and Kug 2002; Choi et al. 2013) and stochastic forcing exerted on the ocean–atmosphere coupled system (Eisenman et al. 2005; Rong et al. 2011). Actually, the dependency of atmospheric deep convection on the underlying SST conditions (Gadgil et al. 1984) provides the most evident nonlinearity, convection anomalies during La Niña being largely displaced westward relative to El Niño. As a result, the associated atmospheric circulation responses in the Northern Hemisphere are approximately shifted by 35° of longitude in phase (Hoerling et al. 1997). Similarly, Wu et al. (2010) demonstrated that the anomalous cyclone over the Philippine Sea during the mature phase of La Niña tends to shift westward, compared with its anticyclonic

Supplemental information related to this paper is available at the Journals Online website: https://doi.org/10.1175/JCLI-D-22-0650.s1.

Corresponding author: Na Wen, wenna@nuist.edu.cn

DOI: 10.1175/JCLI-D-22-0650.1

© 2023 American Meteorological Society. This published article is licensed under the terms of the default AMS reuse license. For information regarding reuse of this content and general copyright information, consult the AMS Copyright Policy (www.ametsoc.org/PUBSReuseLicenses).

Unauthenticated | Downloaded 01/16/25 12:29 PM UTC

counterpart during El Niño. It is also noted that the nonlinear response over the Philippine Sea can lead to asymmetrical evolution of La Niña and El Niño (Ohba and Ueda 2009). Chen et al. (2016) showed that the asymmetric wind stress in the far western tropical Pacific, which is associated with the Philippine cyclone, exerts a distinctive impact on the thermocline evolution at the decaying stage of La Niña. Consequently, La Niña usually displays a weaker decay after its peak and a regain of intensity in the following winter, while El Niño shows a rapid decay and a fast phase transition (Okumura and Deser 2010).

Due to these distinctive features of La Niña, its delayed effect on the subsequent summer monsoonal rainfall in East Asia deserves a comprehensive investigation. The questions to be addressed are the following: How does La Niña influence the following-summer precipitation over East Asia? What is the intermediate SST anomaly in its delay effect? How is the case of La Niña different from El Niño? One further remark needs to be made here about the diversity of ENSO. Based on the spatial location of anomalous SST in the tropical Pacific, El Niño events can be classified into different types (Ashok et al. 2007; Kao and Yu 2009; Kug et al. 2009), and the following-summer precipitation response over East Asia strongly depends on the types of El Niño (Wen et al. 2022, hereafter WLH22). Actually, precipitation anomalies are tightly linked to different intermediate SST anomalies from other oceanic basins while El Niño decays in the tropical Pacific. However, the classification of La Niña events has so far been controversial. Kug and Ham (2011) found the cold events of the ENSO cycle are highly correlated across the central and eastern Pacific, and therefore it is difficult to define prominent types for La Niña. Although Shinoda et al. (2011) separated a certain pattern of La Niña Modoki from normal events with satellite observation, there are very few cases that can be identified. Yuan and Yan (2013) tried to separate the influence of eastern Pacific (EP) La Niña on the tropical atmosphere from that of central pacific (CP; for which the SST anomaly is over the central-eastern equatorial Pacific). But there are many fewer EP La Niña cases that can be identified in mature-phase winter. Using the joint self-organizing map (SOM) analysis, Ashok et al. (2017) also confirmed that types of La Niña are less distinguishable than those of El Niño. In short, there is still a lot of uncertainty about the classification of La Niña, but it is doubtless that SST anomalies of most La Niña cases, particularly the strong ones, are located in the central and eastern equatorial Pacific.

In the present work, we mainly investigate the influence of strong La Niña on East Asian precipitation in the following summer and search for any intermediate SST anomalies that can sustain the delay effect. The paper is organized as follows. Section 2 describes the data and method used. The impact of La Niña on East Asian precipitation in the following summer and the associated regional circulation anomaly are presented in section 3. In section 4, the intermediate SST anomalies that relay the winter La Niña effect into the following summer are identified. Furthermore, the possible mechanisms for the impact of the SST anomaly on atmosphere are also investigated. The observed results are further confirmed by modeling experiments in section 5. Section 6 gives the summary and discussion.

2. Data and methods

a. Observational data and diagnostic method

The observation and model data used in this study are the same as in WLH22. For the sake of completeness, we here give a short description. The precipitation is from the Chinese Meteorological Data Centre, China Meteorological Administration, with a study area (east of 100°E) including 140 stations over East China. To avoid the effect of a strong interdecadal shift taking place at the end of the 1970s, the time period of our investigation is taken from 1979 to 2021. The percentage of precipitation anomaly, which is the ratio of the anomalous precipitation to its seasonal climatological mean, is used to represent its variability. To reduce noise, the precipitation was reconstructed using the first-leading empirical orthogonal function (EOF) mode that retains 70% of the total variance. The monthly SST and atmospheric variables in the same period are from the National Centers for Environmental Prediction–National Center for Atmospheric Research (NCEP–NCAR) reanalysis data (Kalnay et al. 1996) at a grid of 2.5° × 2.5°. All variables are deducted from their mean seasonal cycles and long-term trends.

The composite method is used in this study with the Student's t test (two tail) for evaluating statistical significance. Strong La Niña cases in boreal winter [3-month mean of December, January, and February (DJF0)] are selected for the composite analysis based on Niño-4 index, where the SST anomaly in the region 5°S–5°N, 160°E–150°W is beyond one negative standard deviation. Nine events are selected from 1979 to 2021 (1988/89, 1998/99, 1999/2000, 2000/01, 2007/08, 2008/09, 2010/11, 2011/12, and 2020/21). Through a case-by-case examination, we find that the evolution of the SST anomaly of 2008/09 La Niña and the atmospheric response is very different from other events. To improve the signal-to-noise ratio, we removed this event from the composite analysis. It is to be noted that main conclusions presented in the paper are unchanged, if all La Niña cases during a longer period (1958–2020) are used following the criteria established by the Climate Prediction Center (CPC; https://origin.cpc.ncep.noaa.gov/products/analysis_monitoring/ensostuff/ONI_v5.php).

To investigate the physical mechanism explaining the role of the intermediate SST anomalies in the delay effect of La Niña on atmospheric circulation, as in Wen et al. (2020), we also calculate the wave activity flux as defined by Takaya and Nakamura (2001). The wave activity flux is parallel to the group velocity of the stationary Rossby wave embedded in the mean flow.

b. Model and experiment

To confirm the physical mechanisms deduced from the observation, we leverage the results of existing model experiments, such as the Global Ocean–Global Atmosphere (GOGA) and Pacific pacemaker experiments (Deser et al. 2017), which were

Unauthenticated | Downloaded 01/16/25 12:29 PM UTC

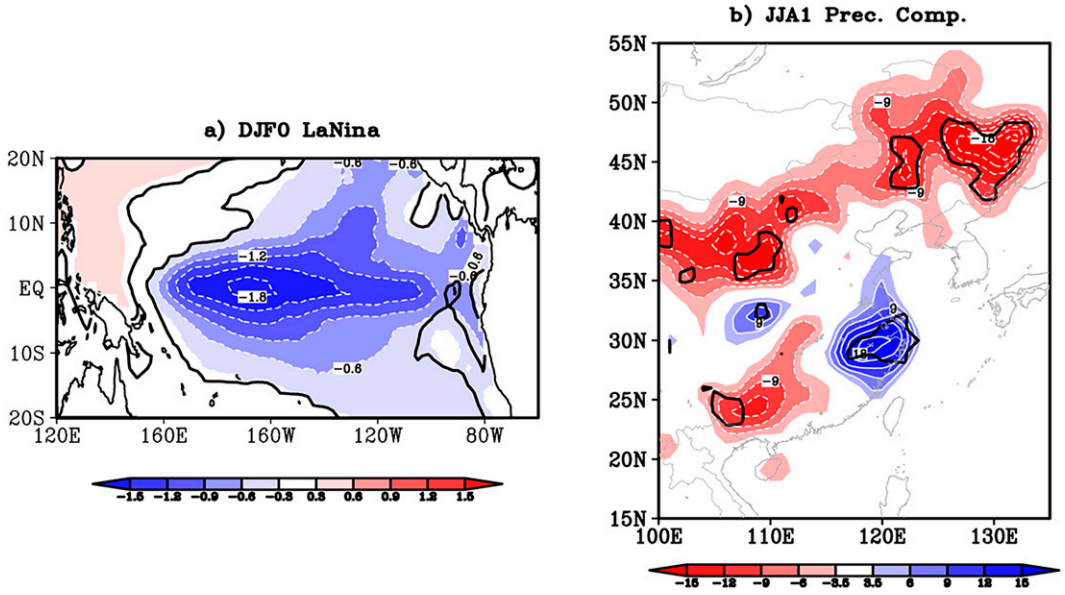

FIG. 1. (a) Composite SST anomaly for La Niña in winter [DJF0; contour interval (CI) = 0.3°C]. Events are selected based on Niño-4 index, where the SST anomaly is beyond a negative standard deviation. (b) Corresponding precipitation anomaly over East Asia (CI = 3%) in its decaying summer (JJA1). The thick black contour denotes the 90% confidence level for precipitation and the 95% confidence level for SST anomalies.

performed by the Climate Variability and Change Working Group (CVCWG; NCAR) using the Community Earth System Model, version 1.1 (CESM1.1). GOGA was conducted using observational SST and sea ice forcing [NOAA Extended Reconstruction Sea Surface Temperature, version 4 (ERSSTv4)], with the Community Atmosphere Model, version 5 (CAM5), the atmospheric component of CESM1.1. The simulation comprises 10 members of different initial conditions, all from 1880 to 2014. The Pacific pacemaker experiment comprises 20 members with CESM1.1. In this pacemaker experiment, the temporal evolution of the eastern tropical Pacific SST (10°S–10°N, 160°–90°W, with a buffer zone extending latitudinally to 20°S and 20°N and longitudinally to 180° and the American coast) is nudged to observations during 1920–2013 (ERSSTv4). This nudging operation maintains the observed evolution of ENSO, while the rest of the coupled system is free to evolve. We use the ensemble mean and process the model output in the same way as we do for observations. The 2020/21 La Niña case is missing in CESM due to its earlier ending of experiment, but our conclusion remains robust if we also exclude the 2020/21 case from our observation diagnosis.

3. Impact of La Niña on East Asian climate

As shown in Fig. 1a, the main body of La Niña is ellipsoidal, mainly covering the Niño-4 and Niño-3.4 regions. Compared to the strong El Niño (typically EP El Niño, such as shown in Fig. 1a of WLH22), the SST anomaly of La Niña is slightly narrower and longer, with the anomalous center westward shifted. The maximal amplitude of the SST anomaly (Fig. 1a) is only 1.5°C, which is much smaller than that of El Niño. These features are consistent with the fact that La Niña and El Niño are generally opposite in sign but show strong asymmetry (Su et al. 2010; Song et al. 2022). The corresponding precipitation anomalies in the following summer show widespread dry conditions over northern and northeastern China. The amplitudes are around 10%–20% of the summer mean precipitation, which pass the 90% confidence level. There are also significantly positive precipitation anomalies along the eastern coast of China and slightly negative precipitation anomalies over southern China (Fig. 1b). This anomalous level, smaller than the counterpart of El Niño (Fig. 1 in WLH22), reveals the relatively weak influence of La Niña on the following-summer precipitation over East Asia. The precipitation pattern is also quite different from that of El Niño, which indicates a different physical mechanism of La Niña influence on the East Asian climate in the following summer.

The precipitation anomaly over East Asia (Fig. 1b) is mainly attributed to an anomalous cyclone over the western tropical Pacific and anomalous high pressure over northeast Asia. As shown in Fig. 2a, there is a pronounced cyclone at 500 hPa with an anomalous center over the South China Sea. It resembles the antiphase of the Philippine Sea anticyclone (Wang and Zhang 2002), which causes the western Pacific subtropical high to retreat eastward by 10° of longitude (as indicated by the dark red dashed line in Fig. 2a). In addition, an anomalous high pressure anomaly is situated in northeast Asia. The low pressure in the south and high pressure in the north create the anomalous easterlies between them, blowing from the western Pacific to eastern-central China. This results in the convergence of water vapor at the junction of land and sea, which corresponds to the precipitation anomalies mainly on the east coast of China (Fig. 2c). However, most areas in

Unauthenticated | Downloaded 01/16/25 12:29 PM UTC

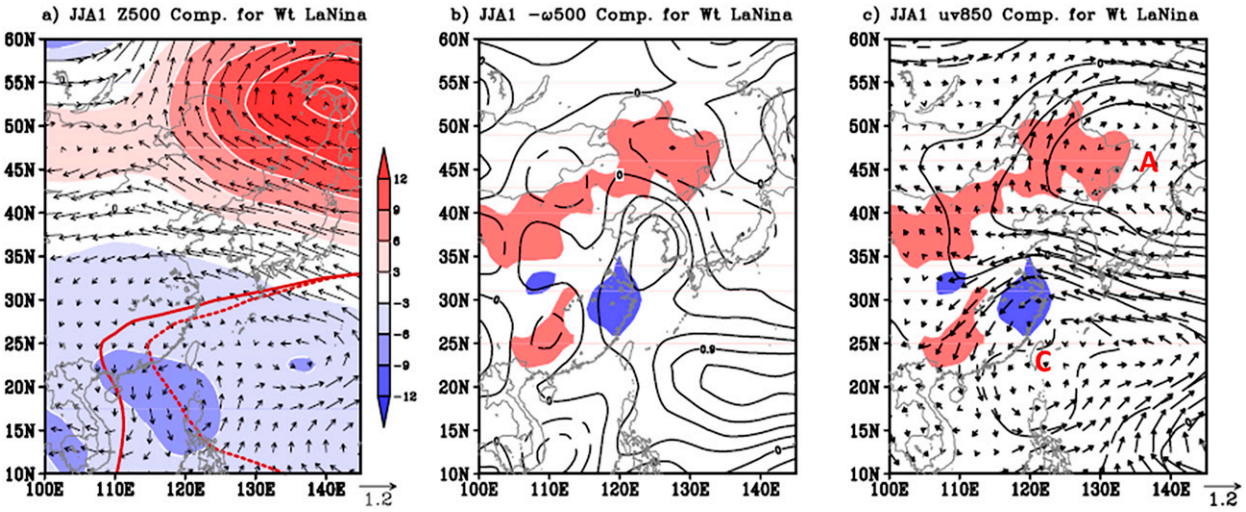

FIG. 2. Composite atmospheric circulation anomalies over East Asia in La Niña decaying summer. (a) 500-hPa geopotential height (shading; CI = 3 m) and wind (vectors; unit: m s^{-1}). The composite (climatological) western Pacific subtropical high is denoted by the 5860-m geopotential height with the thick red dashed (solid) line. (b) 500-hPa vertical velocity ($-\omega$; CI = 0.3×10^{-2} Pa s^{-1}). (c) 850-hPa geopotential height (black contours; CI = 2 m) and wind (vectors; unit: m s^{-1}). The red letters "C" and "A" mark the cyclones and anticyclones, respectively. The shadings in (b) and (c) indicate precipitation anomalies as in Fig. 1b, with blue and red for precipitation anomalies greater than +6% and less than −6%, respectively.

northern and northeast China are in the control of anomalous high pressure. The anticyclone-induced subsidence causes the region to be unusually dry, as indicated by the red shading in Fig. 2b. For southern China, on the northwest flank of the anomalous cyclone, anomalous northeasterly winds prevail (Fig. 2c). Cold and dry airs lead to dry conditions there. Therefore, the cyclone over the western tropical Pacific and the anticyclone over northeast Asia are the key circulations for the precipitation anomaly in Fig. 1b.

4. Intermediate SST anomalies sustaining La Niña delay effect

The subsequent question to address is how winter-peaked La Niña impacts East Asian summer precipitation while it is at its decaying stage with original SST anomalies in the equatorial Pacific very much damped. To address the question, we first use observation data to detect potential intermediate SST anomalies in relation to La Niña in observation, and then investigate the physical mechanisms by which SST anomalies impact the atmosphere.

a. Seasonal evolution of SST anomalies and atmospheric response

Figure 3 displays the evolution of global SST anomalies at La Niña's different stages. Intermediate SST anomalies that can relay the winter La Niña effect into the following summer are probably located over the tropical North Pacific. As shown in Figs. 3a–c, the most pronounced behavior is the evolution of SST anomalies along the west coast of North America. In the mature-phase winter, a narrow zone of cold SST, which is connected to the main body of La Niña in the eastern-central tropical Pacific, propagates northward along the west coast of North America (Fig. 3a). It is strengthened in the subsequent spring, while the main body of La Niña is weakened westward with the anomaly center over the central tropical Pacific (Fig. 3b). In the following summer, the coastal SST anomaly of North America merges with the residual La Niña SST anomaly and forms a prominent Z-shape pattern across the tropical North Pacific (Fig. 3c), which provides a possible "bridge" to connect the winter La Niña with the following-summer precipitation in East Asia. The La Niña–associated SST anomaly along the west coast of North America in Figs. 3a–c is probably due to the adjustment of poleward coastal Kelvin waves (Chelton and Davis 1982) or atmospheric forcing over the tropical North Pacific (Mantua et al. 1997; Schwing et al. 2002). The slightly amplified SST anomalies in the northeast subtropical Pacific (off the coast of California) may also involve local air–sea interactions (Vimont et al. 2003). Besides SST anomalies in the northeast subtropical Pacific, La Niña also induces cold SST anomalies in the tropical Indian Ocean at the mature phase (Fig. 3a). They strengthen in the following spring but almost disappear in the following summer (Figs. 3b,c). Therefore, the tropical Indian Ocean has a minor contribution to the relation of winter-peaked La Niña with the East Asian precipitation in the following summer. Similar results are observed in other oceans, e.g., the SST anomalies in the tropical North Atlantic. Such a configuration suggests that La Niña might mainly rely on the Z-shape SST anomaly in the tropical North Pacific to convey its delayed effect.

Corresponding to such intermediate SST anomalies, the atmospheric circulation at the upper level shows a low pressure belt in the tropics and a clear wave train in midlatitudes. As displayed in Fig. 4a, the entire tropics are dominated by low pressures with an asymmetric pair of Rossby waves across the eastern-central equatorial Pacific at 200 hPa. The larger lobe

Unauthenticated | Downloaded 01/16/25 12:29 PM UTC

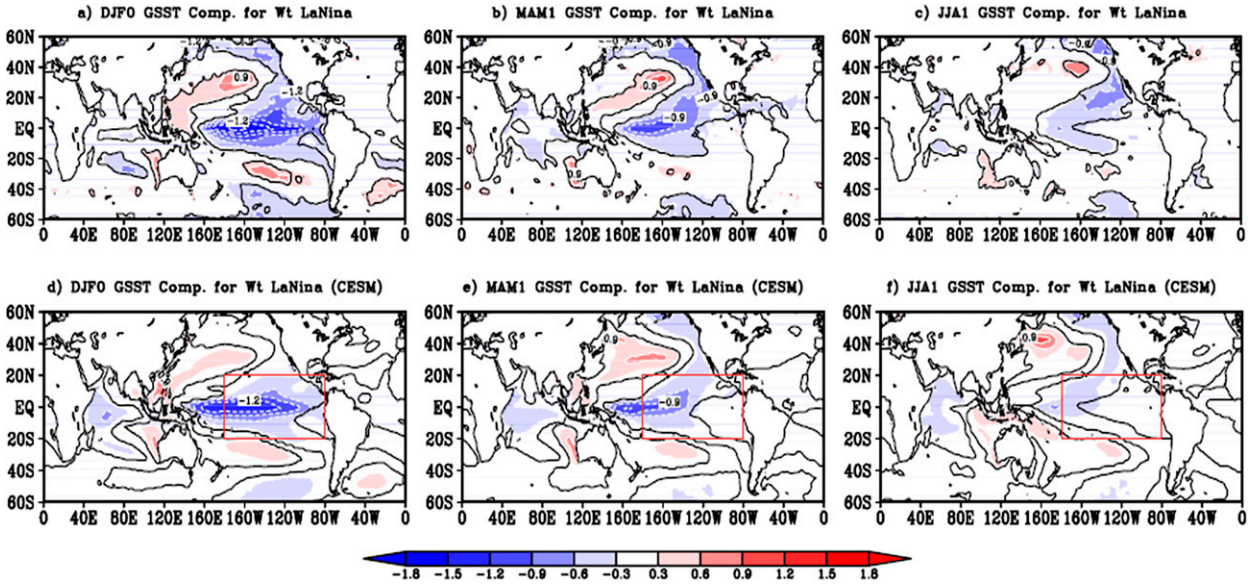

FIG. 3. Evolution of the composite SST anomalies (CI = 0.3°C) for La Niña from (left) its mature winter (DJF0), through (center) the following spring (MAM1), to (right) the decaying summer (JJA1) from the (top) NCAR–NCEP reanalysis data and (bottom) CESM Pacific pacemaker experiment. The thick black contour denotes the 95% confidence level. In the bottom panels, the red box indicates the region 20°S–20°N, 180°–80°W, where SST anomalies are nudged to ERSSTv4 observation.

in the Northern Hemisphere extends its low pressure anomaly eastward to the northern subtropical Atlantic. Consistent with what is observed at the upper level, the atmospheric circulation at 850 hPa shows a clear divergence over the eastern-central tropical Pacific, which results in a descending motion in the midtroposphere and surrounding ascents over the western tropical Pacific and equatorial Atlantic, respectively (Fig. 4b). The configuration of the circulations between the upper and low levels is in line with the atmospheric response to the asymmetric heating about the equator (Gill 1980).

Compared with the tropics, the mid–high-latitude atmospheric response is a clear wave train at the upper level with pronounced anomalous anticyclones over eastern Europe, northeast Asia, the central North Pacific, and northeast Canada, as well as weak anomalous cyclones in between (Fig. 4a). The response amplitudes of the anomaly centers are around 15–30 m, which pass the 90% confidence level. The corresponding low-level wave train in mid–high latitudes (Fig. 4b) indicates the nature of barotropic response. Besides the remarkable zonal wave train at the upper level, there is a meridional wave train along the East Asian coast at low level with an anomalous cyclone over the western tropical Pacific and anomalous anticyclones over northeast Asia–North Pacific (denoted in Fig. 4b). This is consistent with the circulation leading to the East Asian precipitation anomalies in Fig. 2. The meridional wave train is somewhat similar to the Pacific–Japan (PJ) pattern in boreal summer (Nitta 1987) but with a larger scale in the meridional direction.

b. *Possible impact mechanism*

To investigate physical mechanisms by which the intermediate SST anomaly in the tropical North Pacific impacts the atmospheric circulation (as shown in Figs. 4a,b), we first examine the tropical precipitation anomalies in the following summer after La Niña peaks. As shown in Figs. 5a and 5b, the pronounced common feature of both precipitation and OLR is the undulated pattern along the tropical oceans, with deficient rainfalls over the central tropical Pacific and Indian Oceans and abundant rainfalls in the western equatorial Pacific and Atlantic. The last structures are elongated into the north subtropical Pacific and North Africa, respectively. The V-shape negative precipitation anomalies over the central equatorial Pacific correspond well to the tropical part of the intermediate SST anomalies (Fig. 3c) and its associated vertical velocity change in the midtroposphere (Fig. 4b), which indicates the primary role of the intermediate SST anomalies on precipitation. Through the Walker circulation, the SST anomalies lead to positive precipitation anomalies over the tropical Atlantic and the western tropical Pacific, while there are negative precipitation anomalies over the tropical Indian Ocean.

We further investigate the heating-induced convergence and divergence in the atmosphere and the wave activities allowing atmospheric perturbations to propagate across the globe. As shown in Figs. 5c and 5d, cold SST anomalies in the eastern-central tropical Pacific cause local wind divergence at low level and convergence at the upper level. Although the spatial extent of the perturbation is not very large, it is big enough for the perturbation to penetrate into the subtropical jet through the westerly trough over the eastern-central subtropical Pacific. Such as shown in Fig. 5e, the wave activity flux emanates from a positive vorticity over the northeast subtropical Pacific, which corresponds to the asymmetric Rossby wave response to SST anomalies, into the subtropical jet through the channel of the westerly trough (Wen et al. 2019).

Unauthenticated | Downloaded 01/16/25 12:29 PM UTC

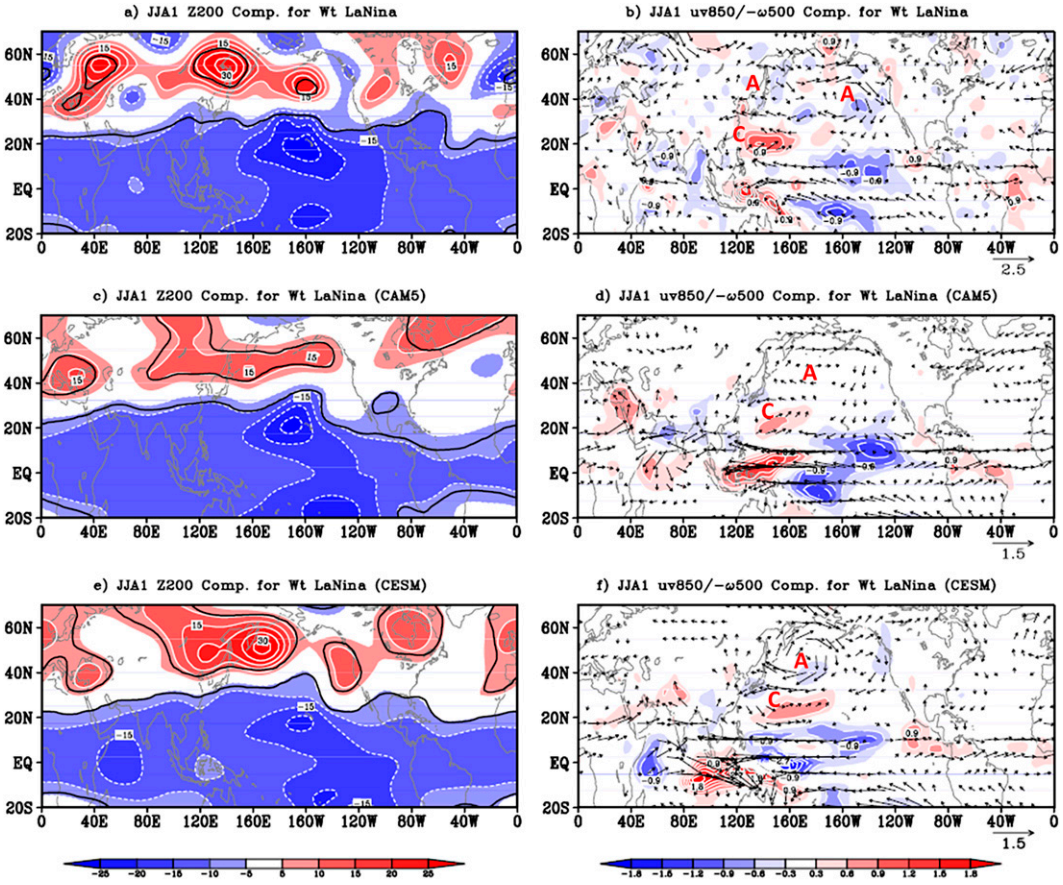

FIG. 4. Composite atmospheric anomalies in La Niña decaying summer derived from (top) the NCEP reanalysis data, (middle) the GOGA experiment of CAM5, and (bottom) the CESM Pacific pacemaker experiment. (left) The 200-hPa geopotential height (shading; CI = 5 m). The black contours denote the 90% confidence level. (right) The 850-hPa wind (vectors; unit: m s^{-1}; omitted if less than one-tenth of the wind vector scalar) and 500-hPa vertical velocity with opposite sign ($-\omega$; shading; CI = 0.3×10^{-2} Pa s^{-1}; ascending in red, descending in blue). The red letters "C" and "A" mark cyclones and anticyclones, respectively.

Due to the waveguide effect of the westerly jet, the perturbation-induced Rossby wave may propagate downstream along the jet, as indicated by the zonal eastward-propagating energy flux (Fig. 5e).

Correspondingly, over the western tropical Pacific, wind converges at the lower level and diverges at the upper level, which results in abundant precipitation there. The divergence center in Fig. 5c is stretched into the far North Pacific, so that perturbations can directly enter the subtropical jet and lead to the wave train response in mid–high latitudes (Wu et al. 2012). More importantly, the perturbation over the western tropical Pacific can excite the low-level meridional-propagating Rossby wave train through the monsoon trough. As shown in Fig. 5f, the energy flux emits from the area of negative vorticity over the western tropical Pacific, which corresponds to the Rossby wave response to the intermediate SST anomalies in low level. It penetrates a zone of positive vorticity over the western subtropical Pacific and continues to propagate into the North Pacific along the westerly jet. Conversely, the energy flux in the upper level propagates southward from northeast Asia to the central subtropical Pacific. The structure of the energy propagation is consistent with that of the PJ pattern (Kosaka and Nakamura 2010), which can be regarded as a dynamical mode of a particular mean state. Under the specific monsoonal circulation background over East Asia, the subtropical anticyclone near the surface and the upper-level subtropical jet constitutes a favorable configuration for the meridional wave (PJ pattern) to gain energy from the mean flow. Although the wave train along the East Asian coast in Fig. 4b is a bit different from the canonical PJ pattern, it can be strongly related to the enhanced convection activities over the Philippine Sea, originally initiated by the intermediate SST anomalies in the eastern-central tropical Pacific. Actually, the easterly and southwesterly wind anomalies, associated with the anomalous anticyclone over the western tropical Pacific (Fig. 4b), strengthen the convergence of the monsoon trough and lead to unusually heavy precipitation over the Philippine Sea (Fig. 5a) and the northward-propagating wave train. This pathway is quite similar to the route from the western

Unauthenticated | Downloaded 01/16/25 12:29 PM UTC

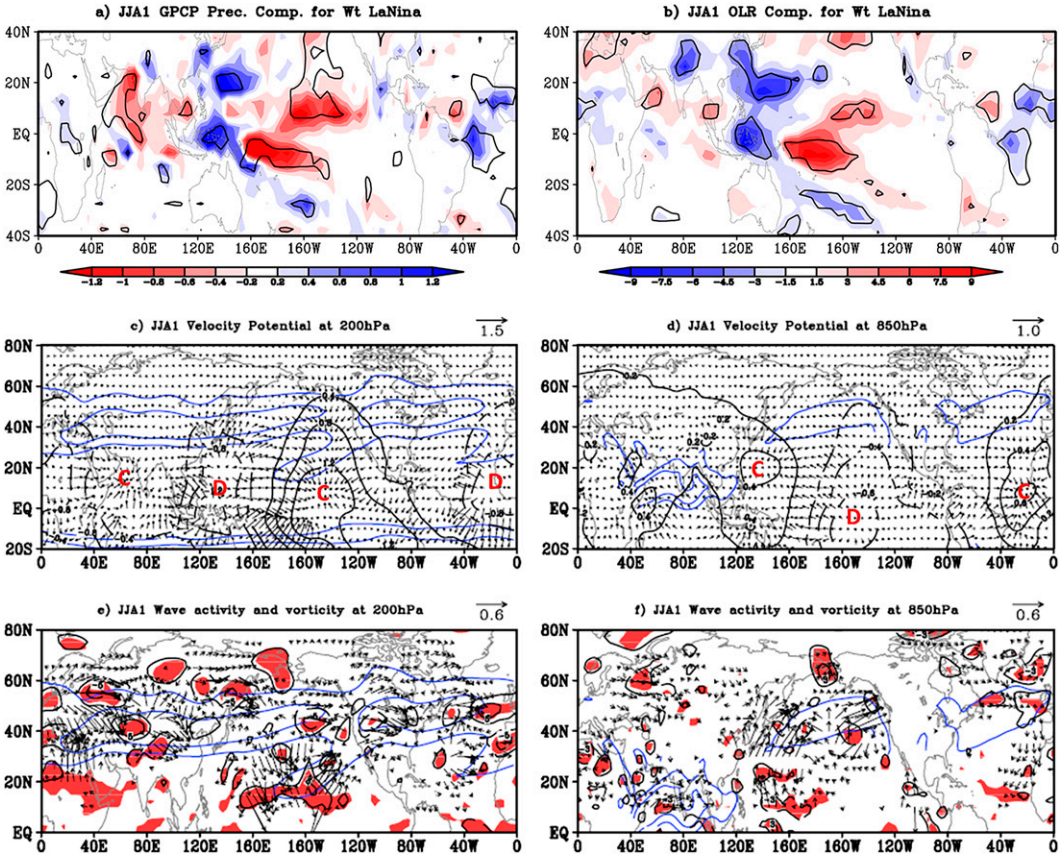

FIG. 5. Composite anomalies from NCAR–NCEP reanalysis data in La Niña-decaying summer. (a) Precipitation (CI = 0.2 mm day^{-1}) and (b) OLR (CI = 1.5 w m^{-2}) with black contours indicating the 90% confidence level. (c),(d) Velocity potential (black contours; 10^6 m^2 s^{-1}) and divergence wind (vectors; m s^{-1}) at 200 and 850 hPa, respectively; red letters "C" and "D" denote convergence and divergence. (e),(f) Wave activity flux (vectors; unit: m^2 s^{-2}; small values omitted if less than one-tenth of the vector scale) and vorticity (black contours; unit: 10^6 s^{-1}) at 200 and 850 hPa, respectively; red shading indicates the 90% confidence level. In (c)–(f), the blue contours denote the climatological westerly wind with speed of 10 and 20 m s^{-1} at 200 hPa and 5 and 10 m s^{-1} at 850 hPa.

tropical Pacific to North America in the persistent year of La Niña (Jong et al. 2020).

In addition to the above two pathways, there is possibly another route by which the intermediate SST anomalies impact the midlatitude circulation. Similar to the western tropical Pacific, there is also a large wind perturbation in the tropical Atlantic. As shown in Figs. 5c and 5d, there is a competing divergence (convergence) in the upper (low) level over the tropical Atlantic–northwest Africa, corresponding to the abnormal precipitation there in Figs. 5a and 5b. Wind disturbances are just at the entrance of the south branch of the subtropical jet over the North Atlantic. They can easily enter the subtropical jet and trigger the downstream wave along the jet. This is clearly evidenced by the energy flux propagation over the eastern tropical Atlantic in Figs. 5e and 5f. In the upper level, the energy flux propagates into the subtropical jet through the westerly trough extending toward the tropical Atlantic. However, in low level, the propagation is southward, opposite to the upper level. It is similar to the energy propagation in the eastern-central subtropical Pacific through the westerly trough over the northeast subtropical Pacific. But there is a significant difference. Perturbations over the eastern-central tropical Pacific are directly induced by the intermediate SST anomalies, while those over the western tropical Pacific and tropical Atlantic–northwest Africa are the results of indirect effects through the Walker circulation.

Although there is convergence over the tropical Indian Ocean in Fig. 5c, the perturbation is weak and mainly confined in the tropics. Therefore, the tropical Indian Ocean does not seem to exert its influence beyond the tropics (Wen et al. 2020). Overall, besides their effect on the tropical low pressure belt through the Kelvin wave adjustment, the intermediate SST anomalies in the tropical North Pacific might affect the midlatitude circulation in three pathways. The first one is through the westerly trough over the eastern-central subtropical Pacific where heating-induced perturbations can easily penetrate the subtropical jet and generate wave train propagation along the jet. The second one is through the western Pacific monsoon trough where atmospheric perturbations can stimulate low-level meridional wave trains along the East

Unauthenticated | Downloaded 01/16/25 12:29 PM UTC

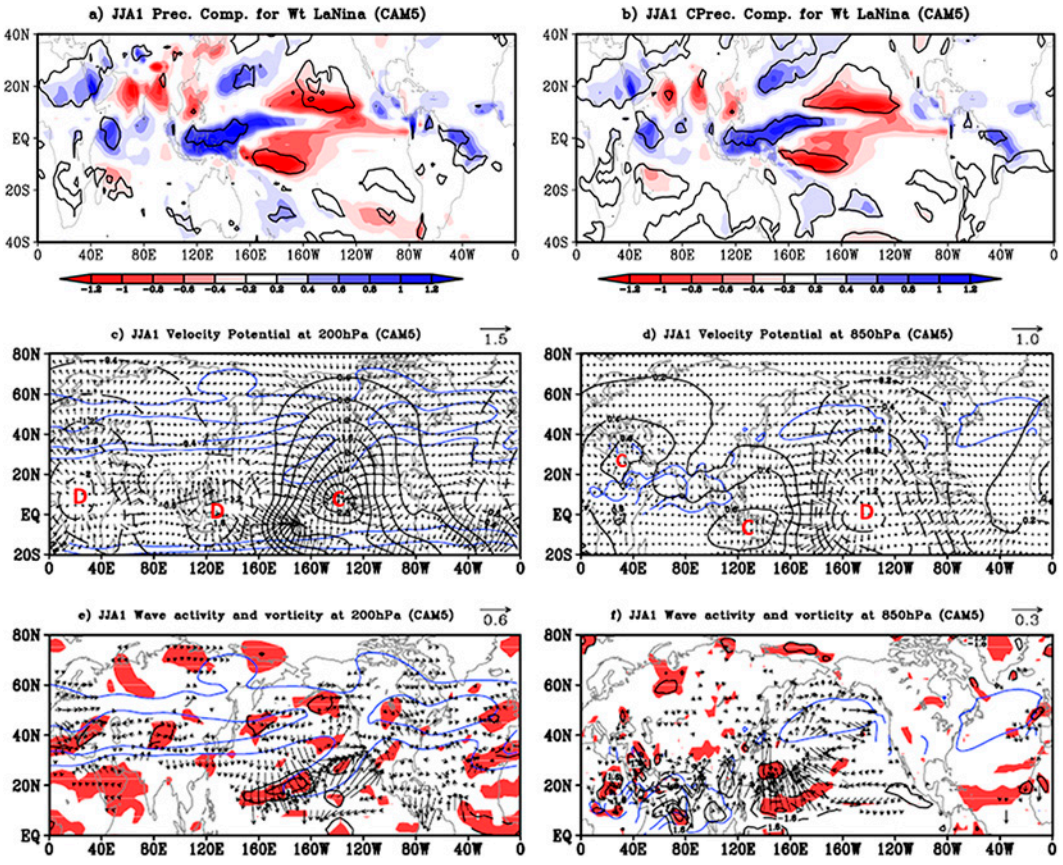

FIG. 6. As in Fig. 5, but for the CAM5 GOGA experiment. (a),(b) Total precipitation and convective precipitation anomalies (CI = 0.2 mm day^{-1}). (c),(d) Velocity potential (black contours; unit: 10^6 m^2 s^{-1}) and divergence wind (vectors; unit: m s^{-1}) at 200 and 850 hPa, respectively. (e),(f) Wave activity flux (vectors; unit:m^2 s^{-2}; small values omitted if less than one-tenth of the vector scale) and vorticity (black contours; unit: 10^6 s^{-1}) at 200 and 850 hPa, respectively. Note that the scale of vectors in (f) is half of that used in (e).

Asian coast. The third one is through the south branch of the North Atlantic subtropical jet that may convey wave propagation in it. These pathways are similar to those of the summer El Niño SST forcing onto the atmosphere in the developing summer (Wen et al. 2019, 2020), although the SST anomaly pattern and position seem very different from the summer El Niño SST anomalies. This may be due to the geographical advantage of the intermediate SST anomalies, especially the SST anomalies in the northeast subtropical Pacific, which is just under the westerly trough over the eastern-central subtropical Pacific.

5. Verification through numerical modeling

In this section, we use existing ocean–atmosphere coupled model simulations to check how observation-based results can be reproduced.

a. GOGA experiment

We first examine the CAM5 GOGA experiment, in which any influence of other underlying surface forcings was excluded and only the effect of SST anomalies was considered. To similar SST forcing as shown in Fig. 3c, the model atmospheric response can well reproduce the observation results in Figs. 4a and 4b. As shown in Fig. 4c, the tropical atmosphere in the upper level presents a low pressure belt response with a pair of asymmetric Rossby waves across the eastern-central equatorial Pacific, which is consistent with the observation in Fig. 4a. The simulated wave train in midlatitudes is relatively weak, but the anticyclonic centers are roughly collocated with the observations, especially for the anticyclone over northeast Asia. At low level, besides the similar tropical atmospheric response, the model can also reproduce the observed meridional wave train, although it is slightly away from the East Asian coast (Fig. 4d). The consistent results between the model and observation consolidate the role and effects of SST anomalies (as shown in Fig. 3c) on atmospheric circulation (Figs. 4a,b).

The model can also simulate the main pathways by which the SST anomaly impacts the atmospheric circulation. As shown in Figs. 6a and 6b, the induced dryness over the central tropical Pacific basically reproduces the observation results, although the pattern is split into two parts with the northern part slightly away from the equator. The surrounding wet

Unauthenticated | Downloaded 01/16/25 12:29 PM UTC

conditions are mainly confined to the equatorial Pacific, which are somewhat different from observations. The corresponding wind shows a dominant convergence at the upper level (Fig. 6c) covering the whole eastern-central tropical and North Pacific, with opposite conditions at low level. The upper-level atmospheric circulation shows a large-scale divergence in North Africa and the tropical Indian Ocean, with a subordinate center in the western tropical Pacific. As a result, there are prominent positive precipitation anomalies over northeast Africa and the western tropical Pacific. These characteristics are slightly different from observations, showing several competing divergences (Fig. 5c) and precipitations (Fig. 5a) over the western tropical Pacific and tropical Atlantic–northwest Africa. Corresponding to the wind perturbation, it is clear that the energy flux over the eastern-central tropical Pacific is effectively transmitted into the subtropical jet through the westerly trough and then propagates downstream along the jet (Fig. 6e). Despite the limited amplitude of the wind perturbation over the western tropical Pacific, there is still the northward propagation wave through the monsoon trough, as indicated by the propagation of energy flux along the coast of East Asia (Fig. 6f). The two pathways are consistent with those observed. However, relative to the observation, the third pathway of the model is slightly shifted to the east of North Africa. As shown in Fig. 6e, the energy flux propagates from North Africa to mid–high latitudes, which corresponds well to the wave train over northern Eurasia (Fig. 4c). That causes perturbations over northeast Africa, which are located on the west side of the South Asian high, and can be transmitted by the southerly wind into the extratropics and stimulate the northeastward-propagating wave in mid–high latitudes (Wang et al. 2005). This is consistent with the findings of Wen et al. (2020) in terms of different types of El Niño influence on the atmosphere. Overall, the model can reproduce the main effect of intermediate SST anomalies on the atmospheric circulation in observation, which enhances our confidence for the proposed physical mechanism.

b. *Pacific pacemaker experiment*

Using the CESM Pacific pacemaker experiment, we demonstrate that winter-peaked La Niña can indeed trigger intermediate SST anomalies in subsequent seasons (spring and summer), as identified in the observation. As shown in Figs. 3d–f, La Niña can initiate SST anomalies along the west coast of North America in winter. They are amplified in the following spring (Fig. 3e) and remain persistent in the following summer (Fig. 3f), which resembles the Z-shape SST anomalies in the tropical northern Pacific in Fig. 3c (observation). However, unlike the observation, the model shows a strong relation of winter La Niña with the basin-scale cold SST in the tropical Indian Ocean, where the SST anomalies generated in winter can be sustained into the following summer. Despite the discrepancies for the simulated SST anomalies in the following summer, CESM can still reproduce the main characteristics of the atmospheric responses in observation. As shown in Fig. 4e, the atmospheric response at the upper level is also a low pressure belt in the tropics with a pair of asymmetric cyclones over the eastern-central tropical Pacific and a salient wave train in midlatitudes. At low level, Fig. 4f also shows a meridional wave train slightly away from the East Asian coast. Compared with GOGA, there are some differences for the pacemaker results, such as the largely amplified anticyclone over northeast Asia–northwest Pacific and enhanced circulation anomalies along the East Asian coast. That might be the joint effect of the SST anomaly forcing over the tropical Indian Ocean. Furthermore, we also examine how the SST anomalies in Fig. 3f exert their influence on the circulation. Despite the interference of the tropical Indian Ocean, the first two pathways of the observations for SST anomalies to affect the atmospheric circulation are clearly simulated (as shown in Fig. 4 of the online supplemental material). This further confirms the bridge role of the SST anomalies in the tropical North Pacific in relaying the winter-peaked La Niña effect into the following summer.

In addition, we also examined the model-simulated precipitation and associated key circulation patterns over East Asia in the following summer after La Niña peaks in boreal winter. As shown in the supplemental Fig. 3, the model can capture the main features of the circulation in Fig. 2, such as the anomalous anticyclone over northeast Asia and the anomalous cyclone over the western subtropical Pacific. But the two key circulations are slightly shifted to the southeast. This results in a southeastward displacement of the entire rainband in the model, relative to the observation in Fig. 1b. Overall, the model results can roughly demonstrate the delayed effect of La Niña on the following-summer East Asian climate through the intermediate SST anomalies identified in Fig. 3.

6. Summary and discussion

This paper aims to investigate impacts of boreal winter–peaked La Niña on the following-summer East Asian precipitation and study how the intermediate SST anomalies can sustain the delayed effect of La Niña on the atmospheric general circulation. Our result indicates that, in the decaying summer [June–August (JJA1)]of La Niña, precipitation shows anomalous dryness in North and South China but anomalous wetness on the east coasts of central China. Such a precipitation pattern is attributed to two key atmospheric circulation structures: the anomalous cyclone over the western tropical Pacific and the anomalous anticyclone over northeast Asia. It is also shown that winter-peaked La Niña affects the East Asian climate in the following summer mainly through intermediate SST anomalies—a Z-shape cold SST over the tropical North Pacific (as shown by the schematic in Fig. 7). It should be noted here that the intermediate SST anomalies actually include the residual SST anomalies of La Niña in the central equatorial Pacific, which can exert direct effect of La Niña's persistence in summer (DiNezio and Deser 2014; Okumura et al. 2017; Song et al. 2022; Anderson et al. 2023).

To the intermediate SST anomaly forcing, the atmospheric circulation shows a low pressure belt response in the tropics due to equatorial Kelvin wave adjustment. In midlatitudes, the atmospheric response presents a zonal wave train in the

Unauthenticated | Downloaded 01/16/25 12:29 PM UTC

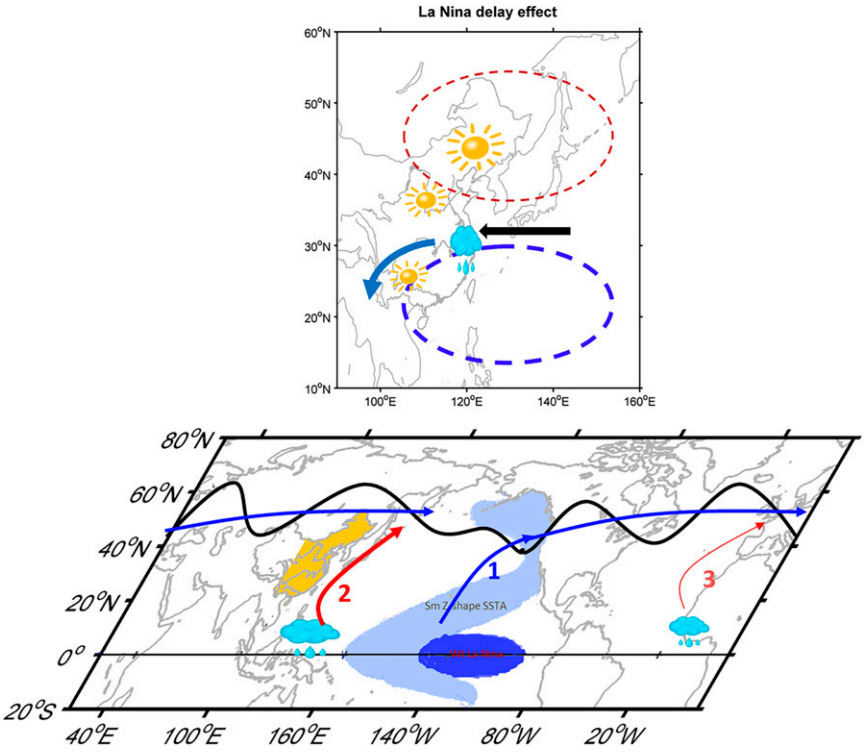

FIG. 7. Schematic showing winter-peaked La Niña impact on the following-summer East Asian precipitation through intermediate SST anomalies in the tropical North Pacific. (top) Precipitation anomalies, together with an anomalous cyclone over the western subtropical Pacific (blue dashed oval) and an anomalous anticyclone over northeast Asia (dark red dashed circle). These precipitation and circulation anomalies are fundamentally caused by the (bottom) winter La Niña–associated intermediate SST anomalies showing a Z shape in the following summer in the tropical North Pacific (light blue shadings). The intermediate SST anomalies exert influence on atmospheric circulation following three pathways. One is near the westerly trough over the northeast subtropical Pacific (blue curve). Another is through the monsoon trough over the western Pacific (red curve). The last one is connected to the south branch of the North Atlantic subtropical jet (light red curve).

upper level and a meridionally propagating wave in low level. Three pathways were suggested for the intermediate SST anomalies to affect the midlatitude atmospheric circulation (as illustrated by the schematic in Fig. 7). One refers to the fact that the SST anomaly–induced perturbations are transmitted into the subtropical jet through the westerly trough over the northeast subtropical Pacific, which in turn stimulates the wave train propagation along the jet. Another is that the SST anomaly–associated perturbations excite the northward-propagating wave along the East Asian coast through the monsoon trough over the western Pacific. And the last one is that the SST anomaly—associated perturbations over the tropical Atlantic—northwest Africa can trigger the downstream-propagating wave through the south branch of the North Atlantic subtropical jet.

To confirm the role of the intermediate SST anomalies and their operating mechanism on atmospheric circulation, we further analyzed the existing GOGA and Pacific pacemaker experiments conducted with CAM and CESM1.1. The model well reproduced the atmospheric circulation anomalies and the first two affecting pathways over the northeast subtropical Pacific and western Pacific. It is also confirmed that the winter La Niña SST anomalies in the eastern-central tropical Pacific can indeed induce the Z-shape cold SST anomaly over the tropical northern Pacific. However, the model generated too-strong, large-scale wind convergence/divergence, and the third pathway in the observation looks much drifted to northeast Africa. The relationship between ENSO and the SST anomalies in the tropical Indian Ocean is also slightly stronger in the model.

In this study, we focused on the recent period of 1979–2020, which is posterior to the climate shift that occurred in East Asia in 1976/77 (Ding et al. 2008). Our choice was intended to avoid possible interference from interdecadal variability. According to Yuan et al. (2014), the influence of La Niña on simultaneous winter precipitation in southern China presented a clear decadal change around 1980. Therefore, the robustness of our findings (including relevant mechanisms) deserves a short discussion in terms of interdecadal variation of the regional climate. Actually, we did prolong our investigation

Unauthenticated | Downloaded 01/16/25 12:29 PM UTC

period and extended it back to 1958. Three strong La Niña events were identified from 1958 to 1978. There are some variations in local precipitation, such as in South China (as shown in supplemental Fig. 1b), which is certainly the manifestation of the interdecadal variation. Despite a few subtle differences, main large-scale characteristics that we present here remain unchanged, such as the widespread anomalous dryness in North China and the anomalous wetness along the east coast of China (properties shown in supplemental Figs. 1b and 2b). It should also be noted that other features in terms of atmospheric circulation, intermediate SST anomalies, and relevant physical mechanisms, have no significant changes (figures not shown). This illustrates the stability and representativeness of our conclusions.

From our analysis, we can see that the intermediate SST anomalies that relay La Niña's delay effect into the following summer are quite different from El Niño (Xie et al. 2016; Li et al. 2017). This can be considered as a manifestation of the asymmetry between the two phases of the ENSO cycle, largely due to nonlinear processes of both ocean and atmosphere (Hoerling et al. 1997; Ohba and Ueda 2009; Chen et al. 2016; Okumura 2019). However, when choosing La Niña index, we find that the circulation response (especially for precipitation anomalies over East Asia) is more sensitive to SST anomalies in the central Pacific than those in the eastern Pacific. This may also be related to nonlinear processes in the atmosphere, in particular, to the threshold issue of atmospheric convection. It implies that La Niña might also need to be typed to study its climate effects in the decaying summer, as is usually the case for El Niño (WLH22). In addition, we can observe many continuous La Niña cases in the past. How the intermediate SST anomalies in the tropical North Pacific contribute to the continuity of La Niña through its induced easterly anomalies in the far western tropical Pacific would be specifically discussed in a separate paper.

Some other issues also need to be addressed in the future. For example, our present study cannot distinguish the propagation modes or regimes within the subtropical jet for the three pathways connecting tropical perturbations to mid- and high latitudes. Further investigation is needed to accurately determine the propagation modes through the use of simplified dynamic models, such as the stationary wave model (Ting and Hoerling 1993) or the linear baroclinic model (Watanabe and Kimoto 2000).

Acknowledgments. This work is supported by the Natural Science Foundation of China (NSFC41475089) and National Key R&D Program of China (2020YFA0608901). Laurent Li acknowledges French GENCI for allocation of computing resources. We are grateful for the editor and three anonymous reviewers for their constructive comments.

Data availability statement. The model simulations presented in section 5 are conducted by the NCAR CESM Climate Variability and Change Working Group. The simulation data are openly available at the website (https://www.cesm.ucar.edu/working_groups/CVC).

REFERENCES

An, S.-I., and F.-F. Jin, 2004: Nonlinearity and asymmetry of ENSO. *J. Climate*, **17**, 2399–2412, https://doi.org/10.1175/1520-0442(2004)017<2399:NAAOE>2.0.CO;2.

Anderson, W., B. I. Cook, K. Slinski, K. Schwarzwald, A. McNally, and C. Funk, 2023: Multiyear La Niña events and multiseason drought in the Horn of Africa. *J. Hydrometeor.*, **24**, 119–131, https://doi.org/10.1175/JHM-D-22-0043.1.

Ashok, K., S. K. Behera, S. A. Rao, H. Weng, and T. Yamagata, 2007: El Niño Modoki and its possible teleconnection. *J. Geophys. Res.*, **112**, C11007, https://doi.org/10.1029/2006JC003798.

——, M. Shamal, A. K. Sahai, and P. Swapna, 2017: Nonlinearities in the evolutional distinctions between El Niño and La Niña types. *J. Geophys. Res. Oceans*, **122**, 9649–9662, https://doi.org/10.1002/2017JC013129.

Chang, C.-P., Y. Zhang, and T. Li, 2000: Interannual and interdecadal variations of the East Asian summer monsoon and tropical Pacific SSTs. Part II: Meridional structure of the monsoon. *J. Climate*, **13**, 4326–4340, https://doi.org/10.1175/1520-0442(2000)013<4326:IAIVOT>2.0.CO;2.

Chelton, D. B., and R. E. Davis, 1982: Monthly mean sea-level variability along the west coast of North America. *J. Phys. Oceanogr.*, **12**, 757–784, https://doi.org/10.1175/1520-0485(1982)012<0757:MMSLVA>2.0.CO;2.

Chen, M., T. Li, X. Shen, and B. Wu, 2016: Relative roles of dynamic and thermodynamic processes in causing evolution asymmetry between El Niño and La Niña. *J. Climate*, **29**, 2201–2220, https://doi.org/10.1175/JCLI-D-15-0547.1.

Choi, K.-Y., G. A. Vecchi, and A. T. Wittenberg, 2013: ENSO transition, duration, and amplitude asymmetries: Role of the nonlinear wind stress coupling in a conceptual model. *J. Climate*, **26**, 9462–9476, https://doi.org/10.1175/JCLI-D-13-00045.1.

Deser, C., I. R. Simpson, K. A. McKinnon, and A. S. Phillips, 2017: The Northern Hemisphere extra-tropical atmospheric circulation response to ENSO: How well do we know it and how do we evaluate models accordingly?. *J. Climate*, **30**, 5059–5082, https://doi.org/10.1175/JCLI-D-16-0844.1.

DiNezio, P. N., and C. Deser, 2014: Nonlinear controls on the persistence of La Niña. *J. Climate*, **27**, 7335–7355, https://doi.org/10.1175/JCLI-D-14-00033.1.

Ding, Y., Z. Wang, and Y. Sun, 2008: Inter-decadal variation of the summer precipitation in East China and its association with decreasing Asian summer monsoon. Part I: Observed evidences. *Int. J. Climatol.*, **28**, 1139–1161, https://doi.org/10.1002/joc.1615.

Dommenget, D., T. Bayr, and C. Frauen, 2013: Analysis of the non-linearity in the pattern and time evolution of El Niño Southern Oscillation. *Climate Dyn.*, **40**, 2825–2847, https://doi.org/10.1007/s00382-012-1475-0.

Eisenman, I., L. Yu, and E. Tziperman, 2005: Westerly wind bursts: ENSO's tail rather than the dog? *J. Climate*, **18**, 5224–5238, https://doi.org/10.1175/JCLI3588.1.

Gadgil, S., P. V. Joseph, and N. V. Joshi, 1984: Ocean–atmosphere coupling over monsoon regions. *Nature*, **312**, 141–143, https://doi.org/10.1038/312141a0.

Gill, A. E., 1980: Some simple solutions for heat-induced tropical circulation. *Quart. J. Roy. Meteor. Soc.*, **106**, 447–462, https://doi.org/10.1002/qj.49710644905.

Hoerling, M. P., A. Kumar, and M. Zhong, 1997: El Niño, La Niña, and the nonlinearity of their teleconnections. *J. Climate*, **10**, 1769–1786, https://doi.org/10.1175/1520-0442(1997)010<1769:ENOLNA>2.0.CO;2.

Unauthenticated | Downloaded 01/16/25 12:29 PM UTC

Hoskins, B. J., and D. J. Karoly, 1981: The steady linear response of a spherical atmosphere to thermal and orographic forcing. *J. Atmos. Sci.*, **38**, 1179–1196, https://doi.org/10.1175/1520-0469(1981)038<1179:TSLROA>2.0.CO;2.

Jong, B.-T., M. Ting, R. Seager, and W. B. Anderson, 2020: ENSO teleconnections and impacts on U.S. summertime temperature during a multiyear La Niña life cycle. *J. Climate*, **33**, 6009–6024, https://doi.org/10.1175/JCLI-D-19-0701.1.

Kalnay, E., and Coauthors, 1996: The NCEP/NCAR 40-Year Reanalysis Project. *Bull. Amer. Meteor. Soc.*, **77**, 437–472, https://doi.org/10.1175/1520-0477(1996)077<0437:TNYRP>2.0.CO;2.

Kang, I.-S., and J.-S. Kug, 2002: El Niño and La Niña sea surface temperature anomalies: Asymmetry characteristics associated with their wind stress anomalies. *J. Geophys. Res.*, **107**, 4372, https://doi.org/10.1029/2001JD000393.

Kao, H.-Y., and J.-Y. Yu, 2009: Contrasting eastern-Pacific and central-Pacific types of ENSO. *J. Climate*, **22**, 615–632, https://doi.org/10.1175/2008JCLI2309.1.

Kosaka, Y., and H. Nakamura, 2010: Mechanisms of meridional teleconnection observed between a summer monsoon system and a subtropical anticyclone. Part I: The Pacific–Japan pattern. *J. Climate*, **23**, 5085–5108, https://doi.org/10.1175/2010JCLI3413.1.

Kug, J.-S., and Y.-G. Ham, 2011: Are there two types of La Nina? *Geophys. Res. Lett.*, **38**, L16704, https://doi.org/10.1029/2011GL048237.

——, F.-F. Jin, and S.-L. An, 2009: Two types of El Niño events: Cold tongue El Niño and warm pool El Niño. *J. Climate*, **22**, 1499–1515, https://doi.org/10.1175/2008JCLI2624.1.

Li, T., B. Wang, B. Wu, T. Zhou, C.-P. Chang, and R. Zhang, 2017: Theories on formation of an anomalous anticyclone in western North Pacific during El Niño: A review. *J. Meteor. Res.*, **31**, 987–1006, https://doi.org/10.1007/s13351-017-7147-6.

Li, Z. X., and S. Conil, 2003: Transient response of an atmospheric GCM to North Atlantic SST anomalies. *J. Climate*, **16**, 3993–3998, https://doi.org/10.1175/1520-0442(2003)016<3993:TROAAG>2.0.CO;2.

Mantua, N. J., S. R. Hare, Y. Zhang, J. M. Wallace, and R. C. Francis, 1997: A Pacific interdecadal climate oscillation with impacts on salmon production. *Bull. Amer. Meteor. Soc.*, **78**, 1069–1080, https://doi.org/10.1175/1520-0477(1997)078<1069:APICOW>2.0.CO;2.

McPhaden, M. J., and X. Zhang, 2009: Asymmetry in zonal phase propagation of ENSO sea surface temperature anomalies. *Geophys. Res. Lett.*, **36**, L13703, https://doi.org/10.1029/2009GL038774.

Nitta, T., 1987: Convective activities in the tropical western Pacific and their impact on the Northern Hemisphere summer circulation. *J. Meteor. Soc. Japan*, **65**, 373–390, https://doi.org/10.2151/jmsj1965.65.3_373.

Ohba, M., and H. Ueda, 2009: Role of nonlinear atmospheric response to SST on the asymmetric transition process of ENSO. *J. Climate*, **22**, 177–192, https://doi.org/10.1175/2008JCLI2334.1.

Okumura, Y. M., 2019: ENSO diversity from an atmospheric perspective. *Curr. Climate Change Rep.*, **5**, 245–257, https://doi.org/10.1007/s40641-019-00138-7.

——, and C. Deser, 2010: Asymmetry in the duration of El Niño and La Niña. *J. Climate*, **23**, 5826–5843, https://doi.org/10.1175/2010JCLI3592.1.

——, P. DiNezio, and C. Deser, 2017: Evolving impacts of multiyear La Niña events on atmospheric circulation and U.S. drought. *Geophys. Res. Lett.*, **44**, 11 614–11 623, https://doi.org/10.1002/2017GL075034.

Peng, S., and J. S. Whitaker, 1999: Mechanisms determining the atmospheric response to midlatitude SST anomalies. *J. Climate*, **12**, 1393–1408, https://doi.org/10.1175/1520-0442(1999)012<1393:MDTART>2.0.CO;2.

Rasmusson, E. M., and T. H. Carpenter, 1982: Variations in tropical sea surface temperature and surface wind fields associated with the Southern Oscillation/El Niño. *Mon. Wea. Rev.*, **110**, 354–384, https://doi.org/10.1175/1520-0493(1982)110<0354:VITSST>2.0.CO;2.

Rong, X., R. Zhang, and T. Li, 2010: Impacts of Atlantic sea surface temperature anomalies on Indo-East Asian summer monsoon-ENSO relationship. *Chin. Sci. Bull.*, **55**, 2458–2468, https://doi.org/10.1007/s11434-010-3098-3.

——, ——, ——, and J. Su, 2011: Upscale feedback of high-frequency winds to ENSO. *Quart. J. Roy. Meteor. Soc.*, **137B**, 894–907, https://doi.org/10.1002/qj.804.

Ropelewski, C. F., and M. S. Halpert, 1987: Global and regional scale precipitation patterns associated with the El Niño/Southern Oscillation. *Mon. Wea. Rev.*, **115**, 1606–1626, https://doi.org/10.1175/1520-0493(1987)115<1606:GARSPP>2.0.CO;2.

Schwing, F. B., T. Murphree, L. deWitt, and P. M. Green, 2002: The evolution of oceanic and atmospheric anomalies in the northeast Pacific during the El Niño and La Niña events of 1995–2001. *Prog. Oceanogr.*, **54**, 459–491, https://doi.org/10.1016/S0079-6611(02)00064-2.

Shinoda, T., H. E. Hurlburt, and E. J. Metzger, 2011: Anomalous tropical ocean circulation associated with La Niña Modoki. *J. Geophys. Res.*, **116**, C12001, https://doi.org/10.1029/2011JC007304.

Song, X., R. Zhang, and X. Rong, 2022: Dynamic causes of ENSO decay and its asymmetry. *J. Climate*, **35**, 445–462, https://doi.org/10.1175/JCLI-D-21-0138.1.

Su, J., R. Zhang, T. Li, X. Rong, J.-S. Kug, and C.-C. Hong, 2010: Causes of the El Niño and La Niña amplitude asymmetry in the equatorial eastern Pacific. *J. Climate*, **23**, 605–617, https://doi.org/10.1175/2009JCLI2894.1.

Takaya, K., and H. Nakamura, 2001: A formulation of a phase-independent wave-activity flux for stationary and migratory quasigeostrophic eddies on a zonally varying basic flow. *J. Atmos. Sci.*, **58**, 608–627, https://doi.org/10.1175/1520-0469(2001)058<0608:AFOAPI>2.0.CO;2.

Ting, M., and M. P. Hoerling, 1993: Dynamics of stationary wave anomalies during the 1986/87 El Niño. *Climate Dyn.*, **9**, 147–164, https://doi.org/10.1007/BF00209751.

Vimont, D. J., J. M. Wallace, and D. S. Battisti, 2003: The seasonal footprinting mechanism in the Pacific: Implications for ENSO. *J. Climate*, **16**, 2668–2675, https://doi.org/10.1175/1520-0442(2003)016<2668:TSFMIT>2.0.CO;2.

Wang, B., and Q. Zhang, 2002: Pacific–East Asian teleconnection. Part II: How the Philippine Sea anomalous anticyclone is established during El Niño development. *J. Climate*, **15**, 3252–3265, https://doi.org/10.1175/1520-0442(2002)015<3252:PEATPI>2.0.CO;2.

——, R. Wu, and T. Li, 2003: Atmosphere–warm ocean interaction and its impacts on Asian–Australian monsoon variation. *J. Climate*, **16**, 1195–1211, https://doi.org/10.1175/1520-0442(2003)16<1195:AOIAII>2.0.CO;2.

Wang, Z., C.-P. Chang, B. Wang, and F.-F. Jin, 2005: Teleconnections from tropics to northern extratropics through a southerly conveyor. *J. Climate*, **62**, 4057–4070, https://doi.org/10.1175/JAS3600.1.

Unauthenticated | Downloaded 01/16/25 12:29 PM UTC

Watanabe, M., and M. Kimoto, 2000: Atmosphere-ocean thermal coupling in the North Atlantic: A positive feedback. *Quart. J. Roy. Meteor. Soc.*, **126B**, 3343–3369, https://doi.org/10.1002/qj.49712657017.

Wen, N., and Y. Hao, 2021: Contrasting El Niño impacts on East Asian summer monsoon precipitation between its developing and decaying stages. *Int. J. Climatol.*, **41**, 2375–2382, https://doi.org/10.1002/joc.6964.

——, Z. Liu, and L. Li, 2019: Direct ENSO impact on East Asian summer precipitation in the developing summer. *Climate Dyn.*, **52**, 6799–6815, https://doi.org/10.1007/s00382-018-4545-0.

——, L. Li, and J.-J. Luo, 2020: Direct impacts of different types of El Niño in developing summer on East Asian precipitation. *Climate Dyn.*, **55**, 1087–1104, https://doi.org/10.1007/s00382-020-05315-1.

——, ——, and Y. Hao, 2022: Response of East Asian summer precipitation to intermediate SST anomalies while El Niño decays and dependence on type of events. *J. Climate*, **35**, 3845–3860, https://doi.org/10.1175/JCLI-D-21-0335.1.

Wu, B., T. Zhou, and T. Li, 2009: Seasonally evolving dominant interannual variability modes of East Asian climate. *J. Climate*, **22**, 2992–3005, https://doi.org/10.1175/2008JCLI2710.1.

——, T. Li, and T. Zhou, 2010: Asymmetry of atmospheric circulation anomalies over the western North Pacific between El Niño and La Niña. *J. Climate*, **23**, 4807–4822, https://doi.org/10.1175/2010JCLI3222.1.

Wu, Z., J. Li, Z. Jiang, J. He, and X. Zhu, 2012: Possible effects of the North Atlantic Oscillation on the strengthening relationship between the East Asian summer monsoon and ENSO. *Int. J. Climatol.*, **32**, 794–800, https://doi.org/10.1002/joc.2309.

Xie, S.-P., K. Hu, J. Hafner, H. Tokinaga, Y. Du, G. Huang, and T. Sampe, 2009: Indian Ocean capacitor effect on Indo-western Pacific climate during the summer following El Niño. *J. Climate*, **22**, 730–747, https://doi.org/10.1175/2008JCLI2544.1.

——, K. Yu, Y. Du, K. Hu, J. S. Chowdary, and G. Huang, 2016: Indo-western Pacific Ocean capacitor and coherent climate anomalies in post-ENSO summer: A review. *Adv. Atmos. Sci.*, **33**, 411–432, https://doi.org/10.1007/s00376-015-5192-6.

Yang, J., Q. Liu, S.-P. Xie, Z. Liu, and L. Wu, 2007: Impact of the Indian Ocean SST basin mode on the Asian summer monsoon. *Geophys. Res. Lett.*, **34**, L02708, https://doi.org/10.1029/2006GL028571.

Yuan, Y., and H. Yan, 2013: Different types of La Niña events and different responses of the tropical atmosphere. *Chin. Sci. Bull.*, **58**, 406–415, https://doi.org/10.1007/s11434-012-5423-5.

——, C. Li, and S. Yang, 2014: Decadal anomalies of winter precipitation over southern China in association with El Niño and La Niña. *Acta Meteor. Sin.*, **28**, 91–110, https://doi.org/10.1007/s13351-014-0106-6.

Zhang, R., A. Sumi, and M. Kimoto, 1999: A diagnostic study of the impact of El Niño on the precipitation in China. *Adv. Atmos. Sci.*, **16**, 229–241, https://doi.org/10.1007/BF02973084.

Zhou, T., W. Bo, and D. Lu, 2014: Advances in research of ENSO changes and the associated impacts on Asian-Pacific climate. *Asia-Pac. J. Atmos. Sci.*, **50**, 405–422, https://doi.org/10.1007/s13143-014-0043-4.

Unauthenticated | Downloaded 01/16/25 12:29 PM UTC